de Haas–van Alphen Study of the Fermi Surfaces of Superconducting LiFeP and LiFeAs

C. Putzke,[1] A. I. Coldea,[2,*] I. Guillamón,[1] D. Vignolles,[3] A. McCollam,[4] D. LeBoeuf,[3] M. D. Watson,[2] I. I. Mazin,[5] S. Kasahara,[6] T. Terashima,[6] T. Shibauchi,[7] Y. Matsuda,[7] and A. Carrington[1,†]

[1]*H. H. Wills Physics Laboratory, University of Bristol, Tyndall Avenue, Bristol, BS8 1TL, United Kingdom*
[2]*Clarendon Laboratory, Department of Physics, University of Oxford, Parks Road, Oxford OX1 3PU, United Kingdom*
[3]*Laboratoire National des Champs Magnétiques Intenses (CNRS), Toulouse, France*
[4]*High Field Magnet Laboratory, IMM, Radboud University Nijmegen, 6525 ED Nijmegen, The Netherlands*
[5]*Code 6393, Naval Research Laboratory, Washington, D.C. 20375, USA*
[6]*Research Center for Low Temperature and Materials Sciences, Kyoto University, Sakyo-ku, Kyoto 606-8501, Japan*
[7]*Department of Physics, Kyoto University, Sakyo-ku, Kyoto 606-8502, Japan*

(Received 25 July 2011; published 26 January 2012)

We report a de Haas–van Alphen oscillation study of the 111 iron pnictide superconductors LiFeAs with $T_c \approx 18$ K and LiFeP with $T_c \approx 5$ K. We find that for both compounds the Fermi surface topology is in good agreement with density functional band-structure calculations and has almost nested electron and hole bands. The effective masses generally show significant enhancement, up to ~3 for LiFeP and ~5 for LiFeAs. However, one hole Fermi surface in LiFeP shows a very small enhancement, as compared with its other sheets. This difference probably results from $\boldsymbol{k}$-dependent coupling to spin fluctuations and may be the origin of the different nodal and nodeless superconducting gap structures in LiFeP and LiFeAs, respectively.

DOI: 10.1103/PhysRevLett.108.047002 PACS numbers: 74.70.−b, 71.18.+y, 74.25.Jb

Identification of the particular structural and electronic characteristics that drive superconductivity in the iron-based materials continues to be a central experimental and theoretical question in the field. A successful theory needs to explain trends, such as the variation of T_c and also the structure of the superconducting energy gap. In most of the iron arsenides the parent materials have a nonsuperconducting, antiferromagnetically ordered ground state. Disruption of this magnetic order leads to superconductivity and then eventually a nonsuperconducting paramagnetic ground state. A good example is the $BaFe_2(As_{1-x}P_x)_2$ series which has a maximum $T_c = 30$ K when $x \simeq 0.33$ [1,2]. Here $BaFe_2As_2$ has a magnetic ground state whereas $BaFe_2P_2$ is a paramagnet and neither superconduct.

The 111 family of iron pnictides $LiFeAs_{1-x}P_x$, is unique because both LiFeAs and its counterpart LiFeP superconduct and are nonmagnetic with $T_c \sim 18$ K [3,4] and ~5 K [5], respectively. Also, penetration depth measurements have shown that LiFeAs is fully gapped [6,7], whereas LiFeP has gap nodes [7]. Establishing whether this switch of pairing structure is linked to changes in the topology and orbital character of the Fermi surface (FS) provides a stringent test of candidate theories for the superconducting pairing in these materials.

Magnetoquantum oscillation effects such as the de Haas–van Alphen (dHvA) effect are a powerful probe of the three-dimensional bulk Fermi surface and have been successfully used to study a variety of iron-based superconductors [8,9]. In this Letter, we present a study of the dHvA oscillations in both LiFeP and LiFeAs which establishes that the *bulk* Fermi surface topology of these compounds is in good agreement with density-functional theory (DFT) calculations. Furthermore, by comparing the values of the extracted effective masses of the quasiparticles to the calculated band masses, we find significant orbit dependence to the mass enhancement factors which is likely linked to the contrasting superconducting gap structures and T_c in these compounds.

Single crystals of LiFeP and LiFeAs were grown by a flux method [10]. Small single crystals, typically $50 \times 50 \times 10$ μm^3 for LiFeP and $100 \times 200 \times 50$ μm^3 for LiFeAs, were selected for the torque measurements. To avoid reaction with air the samples were encapsulated in degassed Apiezon-N grease. Sharp superconducting transitions were measured using radio frequency susceptibility with T_c onset (midpoint) values of 4.9 K (4.7 K) and 18.4 K (17.3 K) for LiFeP and LiFeAs, respectively. The samples were mounted onto miniature Seiko piezoresistive cantilevers which were installed on a rotating platform, immersed in liquid ^{4}He, in the bore of a pulsed magnet up to 58 T in Toulouse. Measurements on the same crystals were also conducted in an 18 T superconducting magnet in Bristol and a 33 T Bitter magnet at HFML in Nijmegen and 45 T hybrid magnet at NHMFL, Tallahassee, all equipped with ^{3}He refrigerators.

Torque versus magnetic field data are shown in Fig. 1. For both materials dHvA oscillations are seen at high fields and low temperatures, well above the upper critical field, estimated to be $\lesssim 1$ T for LiFeP [11] and ~16 T for LiFeAs [12] when $B \parallel c$ (see also Fig. 1). After applying a fast Fourier transform (FFT) as a function of inverse field, several strong peaks are visible (Fig. 1 bottom panels), which correspond to the extremal cross-sectional areas

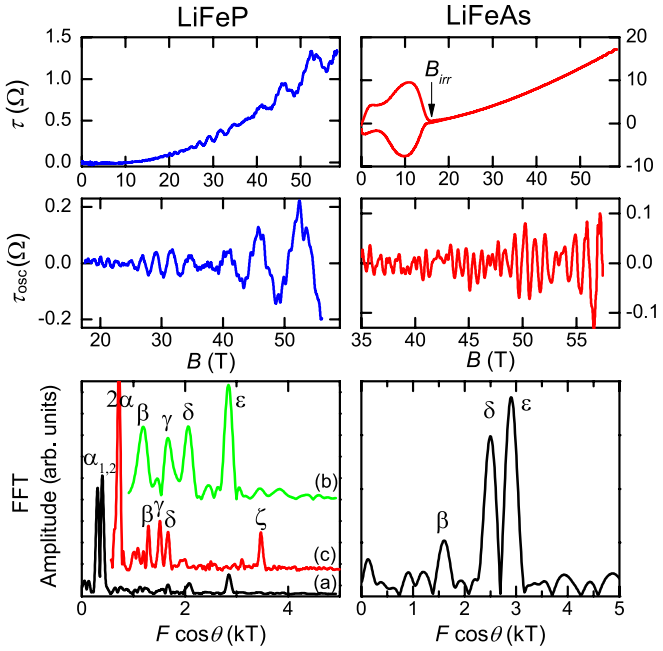

FIG. 1 (color online). Torque versus field for LiFeP and LiFeAs. The top panels show the raw pulsed field torque data in units of the change in the cantilever resistance at $T = 1.5$ K. The arrow indicates the position of the irreversible field. The middle panels show the oscillatory part of the torque after subtraction of a smooth background. The bottom panels show FFTs of the torque. For the peak labels see the main text. For LiFeP we show FFT spectra computed over different field windows (a) (25–58 T) which shows the splitting of the α peaks, (b) (40–58 T) which decreases the influence of noise on the higher frequency peaks, and (c) (33–45 T) for the dc field data at $T = 0.45$ K and $\theta = 51°$, showing the strong ζ peak.

A_k of the FS: $F = \hbar A_k/2\pi e$. For LiFeP, the spectrum is dominated by two low dHvA frequencies around 300 T and 400 T, labeled α_1 and α_2. The amplitude and frequency of the peak at ~750 T are consistent with this being the second harmonic of the α peaks. The other five peaks (β, γ, δ, ε, ζ) are clearly derived from unique Fermi surface orbits. For LiFeAs, three frequencies are visible at 1.5, 2.4, and 2.8 kT, labeled as β, δ, ε, respectively.

To properly identify these FS orbits, we performed field sweeps with different field orientations starting from $\theta = 0°$ ($B\|c$) and rotating towards the ab plane. For a perfectly 2D FS, $F \propto 1/\cos\theta$, so by multiplying F by $\cos\theta$ the degree of two dimensionality of a FS can easily be seen. For quasi-2D surfaces, $F\cos\theta$ will decrease with increasing θ for a local maximum of Fermi surface orbit area as a function of k_z, whereas the opposite will be true for a local minimum. The data in Fig. 2 suggest that for LiFeP ε and γ are a maxima and β and δ are minima. The two lowest frequency α orbits have opposite curvature indicating that they are the maximum and minimum of the same FS sheet. At angles close to $\theta = 50°$ strong peaks are seen (labeled ζ in Figs. 1 and 2) which are likely from the outer hole sheet (band 3). The amplitude becomes large at this angle because of the Yamaji effect, expected when the two extremal orbits of a quasi-two-dimensional Fermi surface cross. Close to $\theta = 30°$, an additional branch η is visible. For LiFeAs, the ε orbit is a maximum, while δ and β orbits are likely to be minima orbits.

To identify the origin of the orbits and solve the structure of the Fermi surface, we have performed DFT calculations using the linear augmented plane wave method, implemented in the WIEN2K package [13]. We used the experimental crystal structure [14] and included spin-orbit coupling (SOC). The calculated Fermi surfaces [see Figs. 2(a) and 2(d)] are quite similar for both materials; there are three hole bands at Γ and two electron bands at M as found previously [15]. The two outermost hole sheets are quite 2D, whereas the innermost $d_{xz/yz}$ hole pocket is strongly hybridized with d_{z^2} near Z and is closed there, while remaining 2D away from this point. By contrast, the electron orbits are very strongly warped. This geometry is reflected in the calculated angular dependence of the dHvA orbits [Figs. 2(b) and 2(c)]. For the 2D hole sheets $F\cos\theta$ varies little with angle and the maximal and minimal area are close. For the electron sheets there is a large deviation from this behavior. For LiFeP, SOC splits the two outermost hole bands, which are accidentally nearly degenerate in nonrelativistic calculations, and causes their character to be mixed $d_{xz/yz}/d_{xy}$. In LiFeAs these bands are well separated irrespective of SOC and have a predominantly $d_{xz/yz}$ (middle) and d_{xy} (outermost) character. The SOC also splits the electron bands along the zone edge (X-M) inducing a gap of ~35 meV [see 2(d)]; hence, as in LaFePO [16], we estimate magnetic breakdown orbits, along the elliptic electron surfaces in the unfolded Brillouin zone, to be strongly damped.

By comparing the calculations to the data [Figs. 2(b) and 2(c)], in particular, the curvature of $F\cos\theta$, the correspondence between the observed dHvA frequencies and the predicted Fermi surface orbits is immediately apparent for most orbits. The observed β frequencies are likely a mixture of signals from orbits $2a$ (hole) and $5a$ (electron) close to $\theta = 0°$ but are separately resolved at angles close to 30° (the η branch probably corresponds to band $5a$). For LiFeP, relatively small shifts (somewhat smaller than for other Fe pnictides [9]) of the band energies, +20 meV and +45 meV for bands 4 and 5 (electron) and −65, −80, 18 meV for bands 1, 2, and 3 (hole), bring the observations and calculations into almost perfect agreement as shown in Fig. 2(b). As in other Fe pnictides [9,17], these shifts shrink both the electron and the hole FSs and likely originate from many-body corrections to the DFT band structure [18]. Although the maximal orbit of band 4, which is close to 6 kT was not observed, probably because the scattering rate in our sample was too high, we can estimate the accuracy of our band energy determinations by calculating the difference in total volume of the electron and hole Fermi

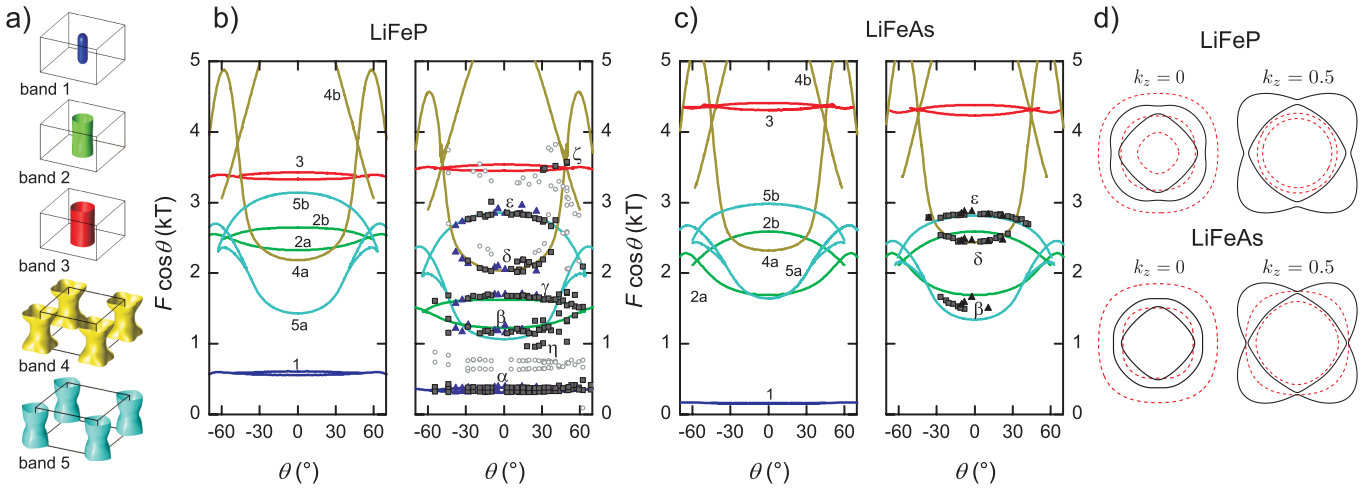

FIG. 2 (color online). (a) Calculated Fermi surfaces of LiFeP. Panels (b) and (c) show the evolution of de Haas–van Alphen frequencies with magnetic field angle. Experimental data are shown in the right-hand panels as symbols (triangles for pulsed field; solid squares for dc field data; open circles for probable 2nd harmonics). The solid lines show the result of the DFT calculations; the bands are shifted in the right-hand panels to best fit the experimental results. The numbers refer to the bands in (a). In all panels the frequencies have been multiplied by cosθ for clarity. (d) Slices through the determined Fermi surfaces at particular k_z values (with shifted bands). The dashed (solid) lines are the hole (electron) sheets, respectively, and the latter have been shifted along the [110] direction such that their center coincides with the holes.

surfaces. We find a small imbalance of just +0.02 electrons per unit cell which shows the consistency of the procedure.

For LiFeAs, the curvature and absolute values of $F\cos\theta$ suggest that the ε orbit originates from the maximum of the inner electron Fermi surface (band 5), and the extended angular dependence of the δ orbit suggests that this originates from the minima of the electron surface (band 4a), rather than the maximum of the middle hole surface (band 2b) which is of similar size in the calculation. The limited angular extent of the data for the β orbit means it is not possible to say if it originates from band 5a (electron) or band 2a (hole) although 5a seems more likely. To accurately match the ε and δ orbits with the calculations, only very small shifts of the band energies are required (-5 and $+18$ meV for bands 4 and 5, respectively) [Fig. 2(b)]. We did not observe the smallest hole FS (band 1) in LiFeAs, even though the same band gave the largest signals for LiFeP. This suggests that band 1 does not cross the Fermi level in LiFeAs, which requires that it shifts down by ~ -40 meV, possibly because of enhanced SOC. The small shift of the electron bands is almost perfectly compensated by the removal of band 1, so the remaining hole bands are not shifted in Fig. 2(b). Although we do not see definitive evidence for the hole orbits, probably because of a significantly higher impurity scattering rate in LiFeAs compared to LiFeP, the small size of the energy shifts needed to match the electron bands combined with the similar small shifts required in LiFeP to match *both* electron and hole bands strongly suggests that the DFT calculations correctly predict the Fermi surface topology of these 111 compounds. This is in contrast to the photoemission results of Borisenko *et al.* [19] for LiFeAs, where a significant discrepancy between the size of the hole sheets and the DFT calculations was found.

The strength of the electron-electron interactions can be estimated from measurements of the quasiparticle effective mass m^* on each orbit through the temperature dependence of the amplitude of the dHvA signals, by fitting the latter to the Lifshitz-Kosevich formula [20] (Fig. 3). These measurements were conducted in dc field on the same samples to avoid any possibility of sample heating at low temperature. The derived values along with the DFT calculations are shown in Table I.

For LiFeP, the enhancements factors $\lambda = m^*/m_b - 1$ vary strongly between orbits. For the electron sheet λ is in the range 1.4–2.3, which is comparable to values found for the electron sheets of LaFePO ($T_c = 6$ K) [21]. The smallest and largest hole sheets (bands 1 and 3) are also strongly

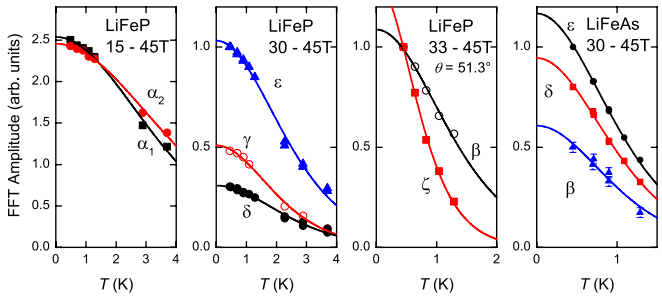

FIG. 3 (color online). Quasiparticle effective masses determination. Amplitude of the FFT peaks (the field ranges as indicated) versus temperature. The lines are fits to the Lifshitz-Kosevich formula [20]. The effective mass values are shown in Table I.

TABLE I. Measured and calculated dHvA frequencies. The measured frequencies are extrapolated to $\theta = 0$ (except those marked with †). The effective (m^*) and calculated (m_b) band masses are quoted in units of the free electron mass (− sign indicates hole orbit). For the LiFeP the values marked with † were determined at an angle of 51° (λ was calculated with m_b also calculated at this angle). At this angle orbits $3a$ and $3b$ cross (and have maximum amplitude), and orbit $2a$ is clearly differentiated from $5a$. Values marked with ♯ potentially have overlapping orbits and so the mass enhancements and orbit assignments are less certain.

LiFeP							LiFeAs						
DFT calc.			Experiment				DFT calc.			Experiment			
Orbit	$F(T)$	m_b	Orbit	$F(T)$	m^*	$\frac{m^*}{m_b} - 1$	Orbit	$F(T)$	m_b	Orbit	$F(T)$	m^*	$\frac{m^*}{m_b} - 1$
1_a	557	−0.44	α_1	316(2)	1.1(1)	1.5(3)	1_a	130	−0.31				
1_b	607	−0.39	α_2	380(2)	1.0(1)	1.6(3)	1_b	149	−0.23				
2_a	2325	−1.7	$\beta^\dagger$	2040(10)†	4.4(1)†	0.6(2)†	2_a	1585	−2.11				
2_b	2645	−1.6	γ	1670(10)	2.7(2)	0.7(1)	2_b	2529	−1.50				
3_a	3328	−1.8	$\zeta^\dagger$	5550(10)†	7.7(2)†	2.1(5)†	3_a	4402	−2.11				
3_b	3428	−1.6	$\zeta^\dagger$	5550(10)†	7.7(2)†	2.1(5)†	3_b	4550	−2.12				
4_a	2183	+0.92	δ	2040(20)	2.2(1)	1.4(2)	4_a	2359	+1.22	δ	2400(25)	5.2(4)	3.3(3)
4_b	6014	+1.8					4_b	6237	+2.34				
5_a	1430	+1.1	$\beta^\sharp$	1160(10)	3.6(2)♯	2.3(2)♯	5_a	1584	+1.54	$\beta^\sharp$	1590(10)	6.0(4)♯	2.9(3)♯
5_b	3142	+0.83	ε	2840(10)	2.2(2)	1.6(3)	5_b	2942	+1.02	ε	2800(40)	5.2(4)	4.1(4)

enhanced; however, for the middle hole sheet (orbits γ and β, band 2) λ is ∼3 times smaller than for the other sheets, despite having similar orbital character. As an enhancement $\lambda \simeq 0.2$ [22] is expected from electron-phonon coupling; this means that the residual electron-electron component for this particular orbit is very weak. This is an interesting observation, relevant to the ongoing discussion [23] as to whether the mass enhancement comes entirely from local correlations or partially from long-range spin fluctuations. If the mass renormalization in this compound is due to the same spin fluctuations that are believed to cause superconductivity, we can conclude that band 2 is very weakly coupled with these fluctuations, so that the pairing amplitude on this band will be small and hence it is a possible candidate for the location of the gap nodes. Calculations suggest [23] that node formation is controlled by the xy pocket, so that if this pocket exists, the order parameter is nodeless, otherwise nodes form on an electron (band 4, in our notation) pocket. LiFeP seems to deviate from this rule, as it has a well-developed xy pocket (band 3) and has gap nodes. LiFeP therefore appears to be a challenging and extremely interesting material for further theoretical modeling.

For LiFeAs, the measured effective masses are uniformly larger than in LiFeP. For the electron sheet (band 5) λ is more than 3 times larger than in LiFeP. This observation suggests that mass renormalization in iron pnictides is caused by the same interaction that drives superconductivity. This agrees with previous findings in the isoelectronic superconducting series, $BaFe_2(As_{1-x}P_x)_2$, in which the effective mass of the electron bands is closely related to the increase in T_c [17]. Interestingly, the large mass enhancement in LiFeAs is not accompanied by a corresponding large shrinking of the Fermi surface volume [17].

In summary, dHvA oscillations have been observed in two members of the 111 family of superconductors, LiFeP and LiFeAs. In both cases we find that measured data are consistent with the topology of the DFT calculated Fermi surface with small band energy shifts. The many-body mass enhancements are larger in LiFeAs than in LiFeP. In LiFeP, the middle hole band has significantly lower mass enhancement than the other sheets, which implies that the electron-hole scatter rate is suppressed for this sheet. This may be the origin of the lower T_c and nodal gap in LiFeP, and suggests that the mass enhancement is to a large extent due to a $\boldsymbol{k}$-dependent spin fluctuations induced interaction, which are also responsible for the pairing. It will be very interesting to see whether these features and the nodal gap structure in LiFeP can be explained by detailed microscopic calculations.

We thank E. Kampert, F. Wolff-Fabris, E. A. Yelland, F. Fabrizi, E. Choi, and A. Bangura for technical assistance and S. Borisenko for discussions. This work is supported by EPSRC (UK), EuroMagNET II under the EU Contract No. 228043, and KAKENHI from JSPS. A portion of this work was performed at the National High Magnetic Field Laboratory, which is supported by National Science Foundation Cooperative Agreement No. DMR-0654118, the State of Florida, and the U.S. Department of Energy.

*Corresponding author.
amalia.coldea@physics.ox.ac.uk
†Corresponding author.
a.carrington@bristol.ac.uk

[1] S. Jiang *et al.*, J. Phys. Condens. Matter **21**, 382203 (2009).
[2] S. Kasahara *et al.*, Phys. Rev. B **81**, 184519 (2010).
[3] J. H. Tapp *et al.*, Phys. Rev. B **78**, 060505 (2008).

[4] M. J. Pitcher *et al.*, Chem. Commun. (Cambridge) **45**, 5918 (2008).
[5] Z. Deng *et al.*, Europhys. Lett. **87**, 37 004 (2009).
[6] H. Kim, M. A. Tanatar, Y. J. Song, Y. S. Kwon, and R. Prozorov, Phys. Rev. B **83**, 100502 (2011).
[7] K. Hashimoto *et al.*, following Letter, Phys. Rev. Lett. **108**, 047003 (2012).
[8] A. Coldea, Phil. Trans. R. Soc. A **368**, 3503 (2010).
[9] A. Carrington, Rep. Prog. Phys. **74**, 124507 (2011).
[10] S. Kasahara *et al.*, arXiv:1112.5597.
[11] K. Mydeen *et al.*, Phys. Rev. B **82**, 014514 (2010).
[12] N. Kurita *et al.*, J. Phys. Soc. Jpn. **80**, 013706 (2011).
[13] P. Blaha, K. Schwarz, G. K. H. Madsen, D. Kvasnicka, and J. Luitz, WIEN2K, edited by Karlheinz Schwarz, Technische Universität Wien, Austria, 2001.
[14] The lattice parameters for LiFeP were determined by x-ray diffraction at 300 K, $a = 3.6955$ Å $c = 6.041$ Å $z_{\mathrm{Li}} = 0.1437$, $z_{\mathrm{P}} = 0.2803$, and for LiFeAs we used $a = 3.7914$ Å $c = 6.3639$ Å $z_{\mathrm{Li}} = 0.1541$, $z_{\mathrm{As}} = 0.2635$ from Ref. [3].
[15] I. R. Shein and A. L. Ivanovskii, Solid State Commun. **150**, 152 (2010).
[16] A. Carrington *et al.*, Physica (Amsterdam) **469C**, 459 (2009).
[17] H. Shishido *et al.*, Phys. Rev. Lett. **104**, 057008 (2010).
[18] L. Ortenzi, E. Cappelluti, L. Benfatto, and L. Pietronero, Phys. Rev. Lett. **103**, 046404 (2009).
[19] S. V. Borisenko *et al.*, Phys. Rev. Lett. **105**, 067002 (2010).
[20] D. Shoenberg, *Magnetic Oscillations in Metals* (Cambridge University Press, Cambridge, England, 1984).
[21] A. I. Coldea *et al.*, Phys. Rev. Lett. **101**, 216402 (2008).
[22] L. Boeri, O. V. Dolgov, and A. A. Golubov, Physica (Amsterdam) **469C**, 628 (2009).
[23] P. J. Hirschfeld, M. M. Korshunov, and I. I. Mazin, Rep. Prog. Phys. **74**, 124508 (2011).